Original Article

Parametric Optimization of Cutting Parameters for Machining of AISI 403 by PVD Coated Tungsten Carbide Inserts Using Taguchi Method

N.N. Jadeja[1], S.H. Zala[2], H.G. Vyas[3], N.D. Mehta[4]

[1,2,3,4]*Department of Mechanical Engineering, Government Engineering College Bhavnagar, Gujarat, India.*

[2]*Corresponding Author : nishazala1979@gmail.com*

Abstract - AISI 403 stainless steel was used for the turning process in our research project. We conducted experiments with various process parameters, including cutting speed, depth of cut and feed to optimize the ideal values for cutting forces FX, FY, and RA. Using an L9 orthogonal array and optimizing output parameters, we studied the performance characteristics of turning with a CNMA120404 carbide insert with a 0.8mm nose radius. We employed the technique of Taguchi during CNC turning to optimize the effects of surface irregularity and cutting forces FX, FY. The use of AISI 403 stainless steel in manufacturing helps to minimize product costs. Our experimental analysis revealed that as speed increases, the total S/N ratio decreases while it increases with feed and cut depth. The optimized values of process factors, such as feed and cut depth, have the greatest influence on surface roughness after cutting speed.

Keywords - Cutting forces, Stainless steel, Surface roughness, Taguchi, S/N ratio, Tungsten carbide inserts.

1. Introduction

Machining is a procedure used to shape metal or other stiff materials by using cutting, grinding, or other processes that require removing metal to achieve precise forms.. Metals are commonly used in various industries, and machining is a common method for shaping them. The tool grips the workpiece. While the cutting tool removes metal through the relative movement between the cutting inserts and the workpiece. For analysis of machining processes, controllable factors are cut of depth, feed, cutting- speed and coating thickness, tool flank wear, tool material, nose radius, etc. Important output factors are surface roughness, cutting force (FX, FY, and FZ), material reduction from the surface, and recovery tool life. Certain angles are crucial when inserting the cutting tool's edge into a workpiece. These angles consist of the lead or entry angle, the radius of the tool nose, the rake angle, the effective rake angle, and the angle of inclination. Various methods of coatings and a variety of coating materials are used like PVD and CVD techniques for coating and coating materials like $TiAiO_2$, $SiAlO_3$, TiNi, and TiZr16.

2. Literature Review

Using multiple response criteria, the Taguchi orthogonal-L9 technique and the Inconel -718 superalloy's end milling operation's different parameters can be assessed using the GRA approach. Nine experimental runs were carried out founded on the L9-orthogonal array of the Taguchi method. Two of the many performance factors taken into account for maximizing cutting speed, feed rate, and cut depth are surface irregularity and material removal percentage. The many aspects of the milling process that are relevant to performance are addressed using a grey relational grade that is derived from a GRA.

The most substantial aspect is also determined by Analyzing Variance (ANOVA). Lastly, to compare the created model with the experimental data, validation tests were run. The outcomes of experiments have established that this strategy has the potential to increase machining performance throughout the final milling process significantly [1]. Trial investigations were carried out with a constant coolant and a 1.5 mm cutting depth in all experimental conditions. These studies investigated the impact of various turning factors and their levels on Ra and calculated the amount of percentage of wear on the cutting tool. The influence of machining factors on VB and Ra was determined using an ANOVA.

Furthermore, Taguchi-based GRA was employed to fix the ideal machining orders for Ra and VB [2]. The Taguchi technique is an essential statistical tool for assessing machining irregularities utilizing cutting parameters such as speed, cut of depth, and feed rate. The minimal machining

surface roughness was examined using the Taguchi technique, the orthogonal array, and the SN ratio [3]. In addition to determining the percentage participation of each parameter, the SN ratio and the ANOVA were utilized to identify the machining parameter that has the biggest impact on surface roughness. To guarantee the authenticity of the test result, a confirmation test was carried out. The findings showed that the levels and combinations of components A2B3C2D1, or the machining carried out with cutting fluid [4].

Experimental results indicate that larger cutting forces, higher temperatures at the chip-tool contact, and lower degrees of surface roughness are seen for tougher workpieces. Surface roughness is more significantly impacted by feed value [5]. The Mean Remaining Life (MRL) of the cutting tool during the machining of Ti-MMCs is assessed using a statistical model created specifically for this project. The initial wear, steady wear, and fast wear regions of the tool wear curve are viewed as separate states by the statistical model [6].

The experiment aimed to measure the tool life of heat-treated AISI-H13 tool steel using P10 and P20 tools. The longest tool life was found in Trial 1 for P20 and Trial 6 for P10, according to the data. To surge the tool life, it is advisable to use a low-cut depth combined with higher cutting velocity [7]. AISI-304 stainless steel and Ti-6Al-4V alloy were tested for machinability utilizing a tapping tester and lubricant in this study. The tapping efficiencies were calculated by comparing three over-based sulfonates with/without sulfurized olefin to a reference lubricant [8]. A recent study that turned hardened D2 tool steel has shown how cutting temperature affects the wear characteristics of carbide tools with a CVD multilayer TiCN/Al2O3 coating and low-content polycrystalline cubic boron nitride tools.

The study highlights how friction kinetics can regulate wear mechanisms in challenging machining conditions [9]. The practical information is analyzed using two methods - the ANOVA and S/N ratio. By conducting the S/N ratio study, the best machining conditions are identified. In contrast, the ANOVA investigation is used to determine the cutting speed's contribution percentage [10]. The project aimed to limit the wear behaviour of a cermet tool material based on Ti (CN) in longitudinal turning.

The study revealed that the qualitative and quantitative characteristics of wear were influenced by the cutting constraints applied and the type of steel used. The three work materials utilized in the research, including two ball-bearing steels and one quenched and tempered steel, had different inclusion contents and microstructures. The three work materials used in the research, including two ball-bearing steels and one quenched and tempered steel, had different inclusion contents and microstructures [11]. This research proposes to enhance our comprehension of the effects that

specific PVD coatings can have on the behaviour of a special material insert when used for turning. An insert for cutting was fabricated using a special material grade that was designed and produced to achieve a high durability level of 8 to 12 [12]. The experimental strategy uses the tool-work thermocouple method, and the theoretical framework is created and verified using the experiment's findings [13].

That sounds like an ambitious and thorough research project investigating the effectiveness of different coatings on cermet tools by examining their mechanical characteristics and surface irregularities, which is crucial for optimizing tool functionality and durability. Developing titanium PVD coatings with varying properties adds another layer of depth to your research, allowing for a direct comparison with existing commercial coatings. The experimental approach will involve the requirements of a tool-work thermocouple method, while the theoretical model will be prepared and authenticated based on the experimental results [14]. To conduct experiments, the L9-orthogonal array based on the DOE was utilized [15].

ANOVA, the level of roughness, and the measured values of SN ratios were used to examine the surface roughness. Based on the investigation, the optimal cutting parameter settings were determined [16]. Examine the presentation of turning operations on AISI 1030 steel bars employing TiN-coated tools utilizing the orthogonal array, the SN ratio, and the ANOVA [17].

In this work, the authors identified a research gap by reviewing the selection of parameters for machining AISISS403. The controlled parameters chosen by the different authors included cutting depth, feed rate, cutting speed, coating thickness, nose radius, flank wear, and coating methods such as PVD and CVD, using various coating materials such as $TiAlO_2$, $TiCN_2$, TiN, $TiAlN$, and $TiSO_3$. The output parameters selected by the authors were SA, FX, FY, FZ, and MRR. After consulting with manufacturing experts and conducting several pilot experiments, selected control parameters are cut depth, federate and speed of cutting; selected output parameters are cutting force Fx, Fy and surface irregularities. The selected insert is Wc, the coating method is PVD, and the coating material is TiZr21.

3. Material Selection

AISISS403 was chosen as the workpiece material for the experiment. Its composition provides impressive mechanical strength. Table 1 shows the composition of material carried out by spectrometry test at the laboratory with spectrometer and SEM analysis done for the finalized percentage of alloy inside workpiece material by NABL test reports. Tungsten carbide inserts were chosen as the material for the inserts, and PVD is the coating method commonly used. The dimensions of the workpiece were 250mm in length and 50mm in diameter. The coating material was selected TiZr21.
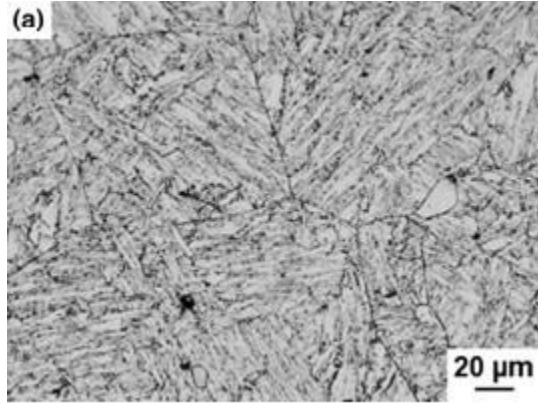
Fig. 1 SEM analysis of AISI SS403

Figure 1 displays the first microstructures of AISISS403. It has a completely martensitic structure with lath diameters larger than 2µm. With typical grain sizes of 100µm, the previous austenite grain boundaries are clearly apparent in the microstructure of AISISS403.

Samples for cylindrical compression measuring 10 mm in height and 8 mm in diameter were made in compliance with ASTM E209 guidelines. During hot compression testing, graphite powder was utilized to minimize lower friction.

The materials utilized in this study was AISISS403, whose chemical compositions are shown in Table 1.

Table 1. Composition of material

Element	Fe	Cr	Mn	Si	C	P	S
Content %	84	11.4	0.98	0.47	0.14	0.038	0.028

The properties of AISI SSS403 stainless steel are recorded in Table 2.

Table 2. Properties of AISI 403 stainless steel

Properties	Metric
Tensile strength	483Mpa
Yield strength	298Mpa
Elastic modulus	189-200Gpa
Poisson's ratio	0.25-0.29
Elongation at break	23.5%
Hardness, Brinell	138
Hardness, Rockwell B	79

4. Experimental Setup and Procedure

For the machining of AISISS 403 stainless steel workpiece material, the HMC lathe machine MONO 200XL type was used. CNMG100414 type tool holder was selected for machining. Figure 2 shows the tester for the surface roughness - ITI surf test RS 232" (make: ITI, India).

Fig. 2 Surface roughness tester

Measure value of cutting forces in FX and FY directions piezoelectric type tool dynamometer is used. There are three frequently used SN ratios: Nominal-is-Better (NB), minimum-is-better (LB), and maximum-is-better. Taguchi, is a valuable approach to designing high-quality production systems optimized using the GRA.L9 orthogonal-array was designed by Taguchi and GRA. The findings show that ultrasonic amplitude, static force, and feed rate have the greatest effects on mechanical qualities [18].

The optimal ratio is determined based on the quality criteria of the product. The current experiment aimed to determine the ideal cutting velocity (Vc), feed rate (f) and cut depth.To obtain ideal surface roughness (Ra value) and minimize the properties of cutting forces. Table 3 displays three 3-levels of parameter segmentation. The Taguchi technique was applied to create machining parameter combinations using an L9-orthogonal array. Taguchi's approach involves designing Orthogonal Arrays (OA) to analyze process constraints in limited tests.

Table 3 presents parameters selected from a literature review and pilot experiments to establish the range for the experiment. Speed of cutting, feed rate, and cut depth are all controlled characteristics. SA, FX, and FY are three output characteristics. Cutting speed is recorded in rpm, feed in mm/rev, and cut of depth in mm. The experimental findings with the SN ratio are examined using the Taguchi approach and MINITAB-19 software.

Table 3. Experimental factors

No.	Factors	Unit	Level-1	Level-2	Level-3
1	C.S.	r.p.m.	550	650	700
2	F.	mm/rev	0.2	0.3	0.4
3	D.O.C.	Mm	0.25	0.35	0.45

5. Experimental Analysis

Table 4 below shows the selected input parameters, which include C.S., F, and D.O.C, and output parameters.

Table 4. Results were examined by the Taguchi technique

Sr.No	C.S	F.	D.O.C.	RA	FX	FY
Unit	r.p.m	Mm/rev	mm	µm	N	N
1	500	0.2	0.25	0.531	154.21	196.3
2	500	0.3	0.35	0.426	55.43	92.45
3	500	0.4	0.45	0.325	68.91	107.9
4	650	0.2	0.35	0.862	119.37	189.3
5	650	0.3	0.45	0.456	112.65	236.8
6	650	0.4	0.25	1.364	94.28	152.05
7	700	0.2	0.45	0.845	118.36	199.5
8	700	0.3	0.25	0.654	100.37	141.5
9	700	0.4	0.35	0.984	35.21	74.1

*C.S .-Cutting speed, F-Feed,D.O.C.-Depth of Cut

5.1. Surface Roughness (RA) Result Analysis

The SN ratio was applied to analyse the outcomes of surface roughness RA using Minitab software. The SN ratios for the Roughness (RA) experiment were calculated using an equation with "smaller the better" measures. The examined SN ratio is utilized for conducting ANOVA. From Figure 3(a), the best value for RA is obtained at 700r.p.m. c.s., f. is 0.4 mm/rev, and d.o.c. is 0.25mm. Figure 4 shows the counter effects of c.s. and f. on surface -roughness. Response Table 5 displays the impact of input parameters on surface roughness. The most significant characteristic is cutting speed, which has a value of 700r.p.m. as shown in Figure 3(b) and is also represented in the response table at rank 1 and level 3. Then,

after the effect of cut depth is important compared to feed. Table 6 presents an analysis of variance that reveals that cutting speed has the greatest effect on Roughness (RA), with a contribution of p-value less than 0.05.

Table 5. Response matrix for RA

Level	Cutting-Speed	Feed	Cut Depth
1	7.557	2.750	2.163
2	1.805	5.974	2.947
3	1.764	2.402	6.015
Delta	5.794	3.572	3.852
Rank	1	3	2

Table 6. Analysis of RA by ANOVA for SN Ratios

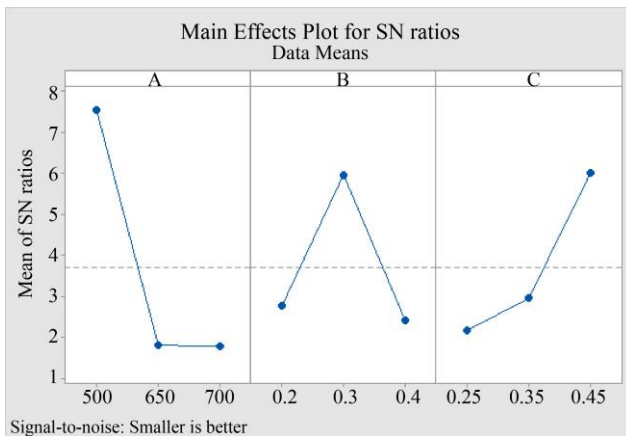| Source	D.F	Seq- SS	Adj-SS	Adj-MS	F-value	P-value
C.S.	2	66.66	66.66	33.330	5.09	0.0242
F.	2	23.27	23.27	11.634	1.78	0.3460
D.O.C.	2	24.86	24.86	12.432	1.90	0.0353
Residual Error	2	13.11	13.11	6.554		
Total	8	127.90				

Fig. 3(a) Signal-to-noise effects on surface roughness
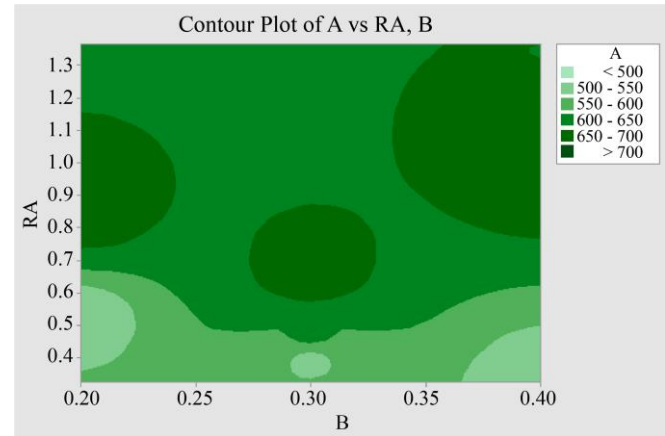
Fig. 3(b) Contour effects on the surface of roughness

Table 7. Model of summary

S	R-squre	R-squre(adj)
0.2459	96.14%	94.56%

ANOVA gives the best model for RA in Table 7 rate of the determination of coefficient R-Squreis 96%, which is more than the R-Squre (adj)rate of the coefficient of determination, which shows an adequate model for surface-roughness.

5.2. Analysis of Cutting Forces
5.2.1. Cutting Force (Fx) Result Analysis

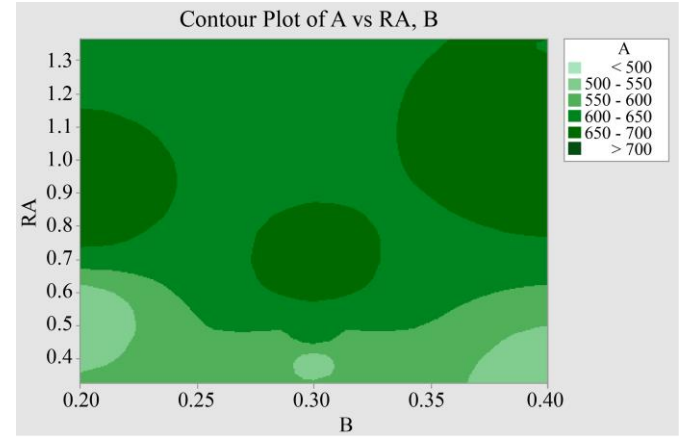The SN ratio was utilized to examine the effects of cutting force FX with Minitab software. The SN ratios for the cutting force Fx trials were computed using a formula with the "smaller the better" standard. The examined SN ratio is applied for ANOVA.

According to Figure 4, the finest value for the cutting force Fx is achieved at a speed of cutting of 700 revolutions per minute, a feed rate of 0.4 mm per revolution, and a depth of cut of 0.35mm. The cutting speed is the most substantial factor that influences the value of the cutting force Fx. The contour effects of feed rate and cutting speed on the cutting force Fx are displayed in Figure 5.
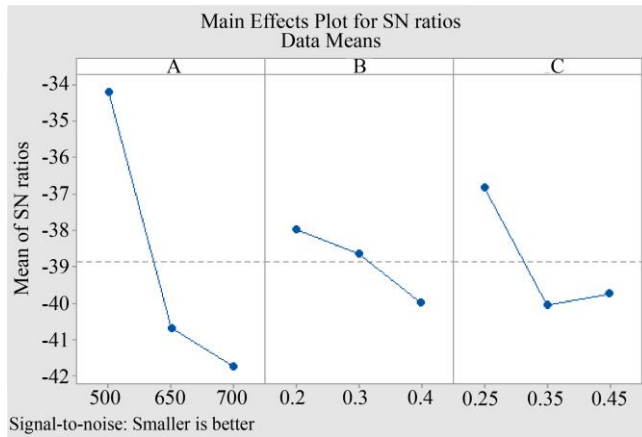
Fig. 4 Signal-to-noise effects on C.F.(FX)

Fig. 5 Contour effects on cutting force FX

Table 8. Response table for FX

Level	Cutting Speed	Feed	Depth of Cut
1	-34.19	-37.98	-36.82
2	-40.69	-38.65	-40.06
3	-41.76	-40.01	-39.75
Delta	7.57	2.03	3.24
Rank	1	3	2

The effect of input factors on surface roughness is shown in Table 8. Speed of cutting is the most dominant parameter, as made known in the figure above with a value of 700r.p.m. This is also reflected in the response table, where it ranks first with a level of 3. The depth of cut has a momentous effect after cutting speed, followed by feed. Table 9 includes an analysis of variance, this shows that, with a contribution of a p-value below 0.05, speed of cutting has the most impact on cutting force (FX). Table 10 shows that the best technique for estimating cutting force (FX) is ANOVA. The coefficient of determination R-Sq is 98.87%, which is higher than the R-Sq (adj) value. This indicates that the model is appropriate for predicting SA.

Table 9. Analysis of Fxby ANOVA for SN Ratios

Source	D.F	Seq SS	Adj SS	Adj MS	F-Value	P-Value
C.S	2	100.575	100.575	50.2873	69.49	0.014
F.	2	6.427	6.427	3.2137	4.44	0.184
D.O.C.	2	19.246	19.246	9.6228	13.30	0.070
Residual Error	2	1.447	1.447	0.7236		
Total	8	127.695				

Table 10. Model of summary

S	Rsqure	Rsqure (adj)
0.8507	98.87%	95.47%

Fig. 6 Signal-to-noise effects on C.F.(FY)
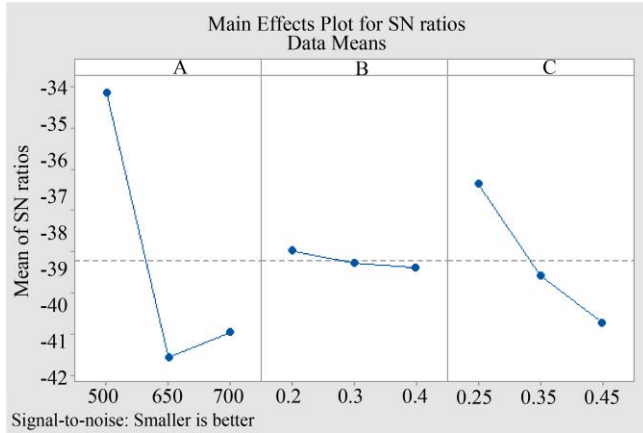
Fig. 7 Contour effects on cutting force FY

Table 11. Response table for FY

Level	Cutting Speed	Feed	Depth of Cut
1	-39.12	-42.98	-41.35
2	-45.56	-43.27	-43.57
3	-44.96	-43.39	-44.72
Delta	6.43	0.41	3.37
Rank	1	3	2

5.2.2. Cutting Force (Fy) Result Analysis

An analysis was conducted using Minitab software to analyze the cutting force FY with the SN ratio. The SN ratio was calculated for the cutting force FY experiments using an equation with the "smaller the better" criteria. The calculated SN ratio was then utilized in the ANOVA.

Figure 6 reveals that the ideal cutting force Fy is achieved at a 650 r.p.m. cutting speed, feed rate of 0.4 mm/rev, and depth of cut is 0.45 mm. Cutting speed is the most substantial factor affecting the value of Fy. Contour effects of feed and on cutting force Fy are illustrated in Figure 7.

The effect of controlled parameters on cutting force FY is shown in Table 11. Speed of cutting is the most crucial parameter, with a value of 650r.p.m. (as given away in Figure 5) and is ranked 1 at level 2 in the response table. Feed and depth of cut are the next important parameters in that order. Table 12 presents an ANOVA that confirms cutting speed's significant influence on cutting force (FY), with a p-value below 0.05.

Table 12. Analysis of Fy by ANOVA for SN Ratios

Source	DF	Seq SS	Adj SS	Adj MS	F-value	P-value
C.S.	2	75.7453	75.7453	37.8727	122.19	0.008
F.	2	0.2647	0.2647	0.1324	0.43	0.701
D.O.C.	2	17.5707	17.5707	8.7854	28.34	0.034
Residual Error	2	0.6199	0.6199	0.3100		
Total	8	94.2007				

Table 13. Model summary

S	R-Sq	R-Sq (adj)
0.8507	99.91%	99.63%

Based on Table 13, it can be decided that ANOVA is the best model for predicting cutting force (FY). This is due to the fact that the R-Sq coefficient of determination (99.91%) is greater than the R-Sq(adj) corrected coefficient of determination. This indicates that the model is fit for expectingcutting force FY accurately.

6. Regression Analysis of Controlled Parameter by MINITAB-19

Regression models were developed for individually controlled factors separately for TiZr21 PVD-coated WC
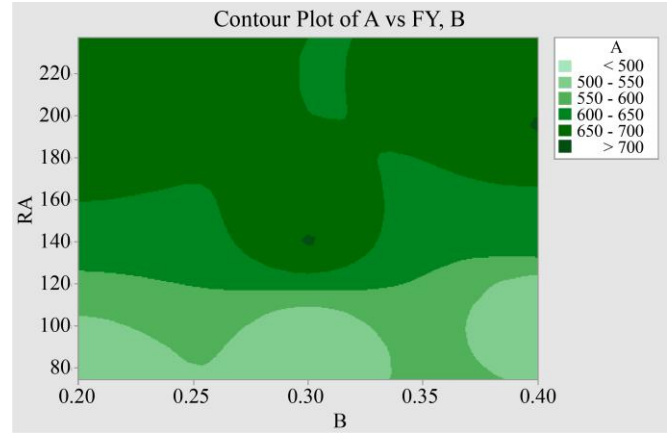
inserts. Developed models are used for the prediction and validation of the experiments.

6.1. Confirmation Experiments for TiZr21 PVD Coated WC Inserts

The L9- orthogonal technique is the best factorial method for reducing the number of experiments and saving time and cost for best results. Here, the experiments of confirmation results are compared with practical and theoretical results shown in Table 14. It was determined that the model had an error of less than 10%. We conducted experiments using an optimal set of parameters for RA, FX, and FY, obtaining optimized values using the L9-Orthogonal method. We repeated the experiments for each set of parameters. This regression analysis shows that the errors found are less than 10%, indicating that each set of parameter pairs for RA, FX, and FY is optimal.

Table 14. Regression mathematical models

C.S	F.	D.O.C	Exp.RA	Pred RA	Error%
Confirmation for RA					
700	0.4	0.25	0.76	0.72	1%
700	0.4	0.35	0.96	0.93	1.5%
650	0.4	0.45	1.56	1.54	2%
Confirmation for Fx					
C.S	F.	D.O.C	Exp. FX	Pred FX	Error%
700	0.4	0.25	30.28	29.45	2%
700	0.4	0.35	30.27	28.56	1%
650	0.4	0.45	29.54	28.56	2.3%
Confirmation for Fy					
C.S	F.	D.O.C	Exp. FY	Pred FY	Error%
700	0.4	0.25	86.58	89.21	4%
700	0.4	0.35	100.21	99.32	5.8%
650	0.4	0.45	250.3	274.4	3%
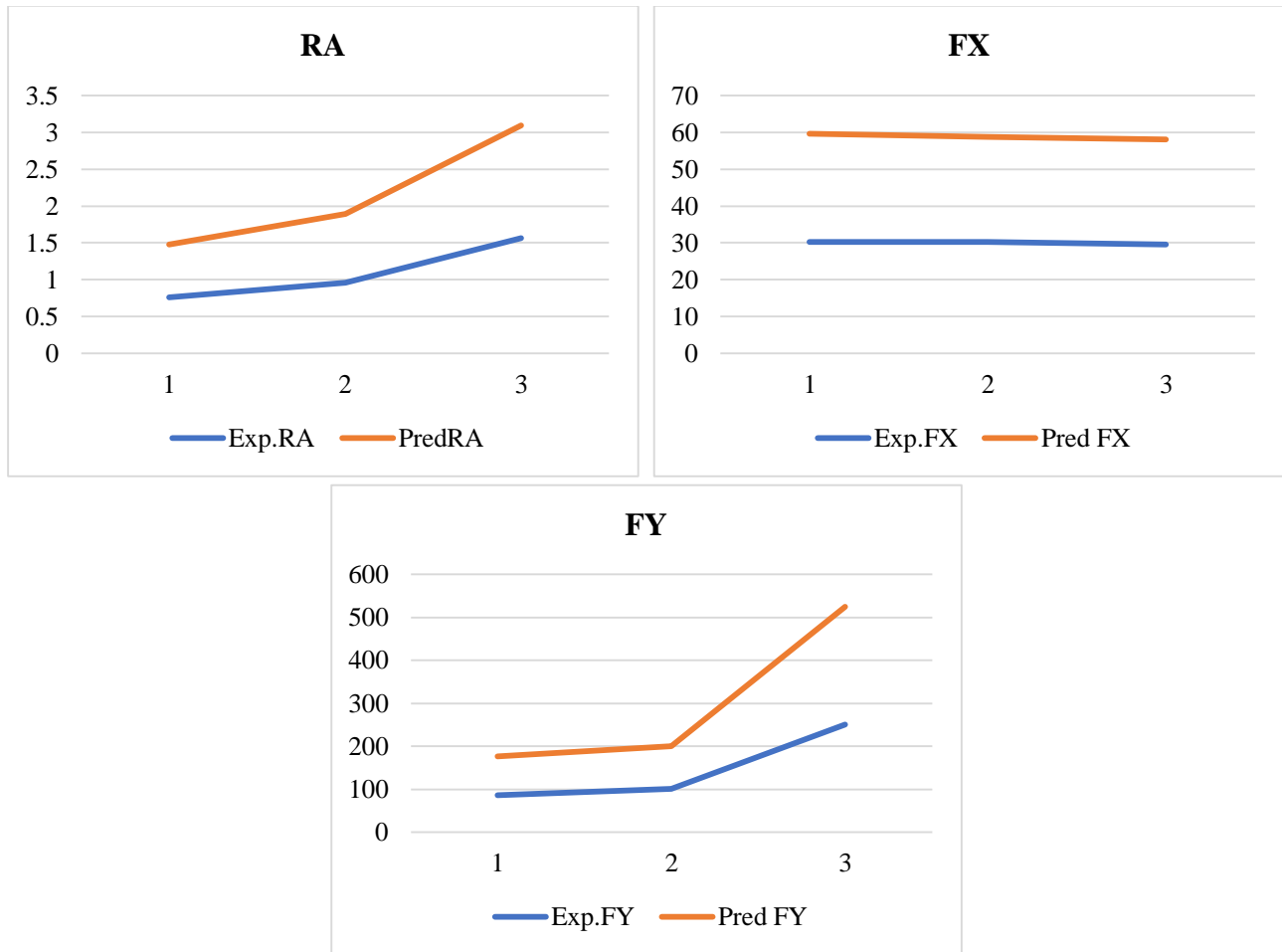
Fig. 8 Confirmation experiments comparisons for RA, FX and FY
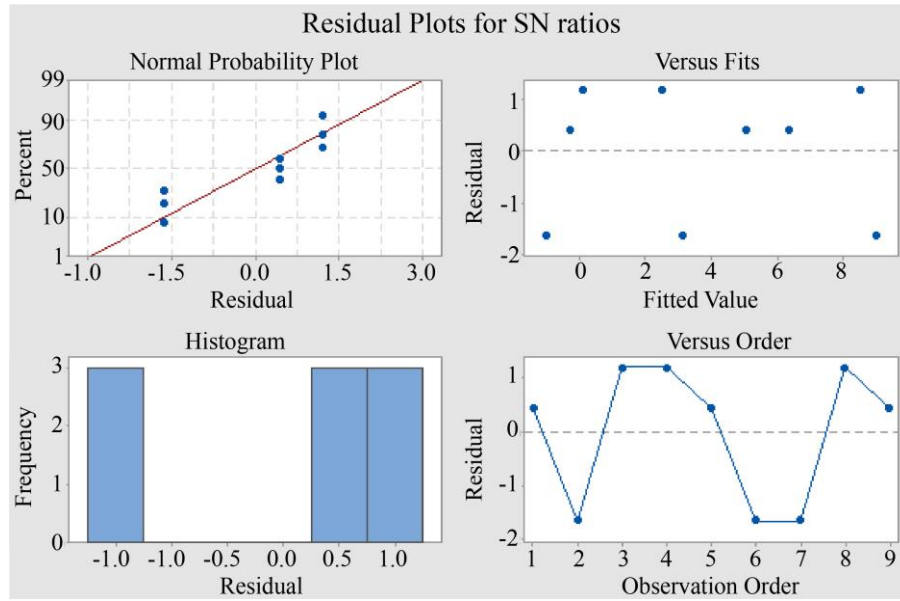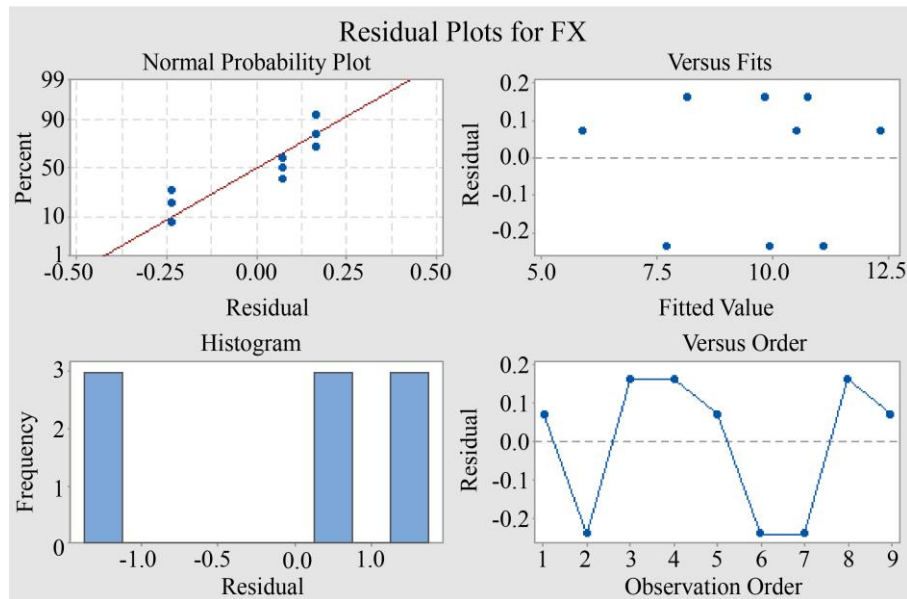
Fig. 9 Residual effects on RA

Fig. 10 Residual effects on FX

Figure 8 shows that the optimum pair of C.S., F. and D.O.C. find out for RA is 700r.p.m., 0.4 mm/rev and 0.25mm. The optimum pair of FX is 700r.p.m., 0.4 mm/rev and 0.35mm with less error 1%, and optimum values for FY are 650r.p.m., 0.4 mm/rev and 0.35mm. Optimizing values for cutting forces Fx reduces friction and flank wear in between tool inserts and workpieces.

Reduced values of Fx can reduce power consumption during turning of AISI SS 403. The residual plot below displays the number of combinations that have interaction plots between various input responses. The total number of interaction combinations is shown in the graph. Figures 9, 10 and 11 show different residual effects for SA and cutting forces FX and FY. The residual line is followed by the optimal reading points from 9 experiments. Controlled factor results were available within vs fit to model, indicating a constant residual variance.

Residuals are usually distributed, as observable from the probability plot and histogram, and they move around a continuous mean. As a result, the regression model's assumptions are satisfied. The results of the regression analysis of Ra and FX, FY indicate that speed of cutting and feed are the most important components. The set of output responses yields the best answer for the controllable factors.
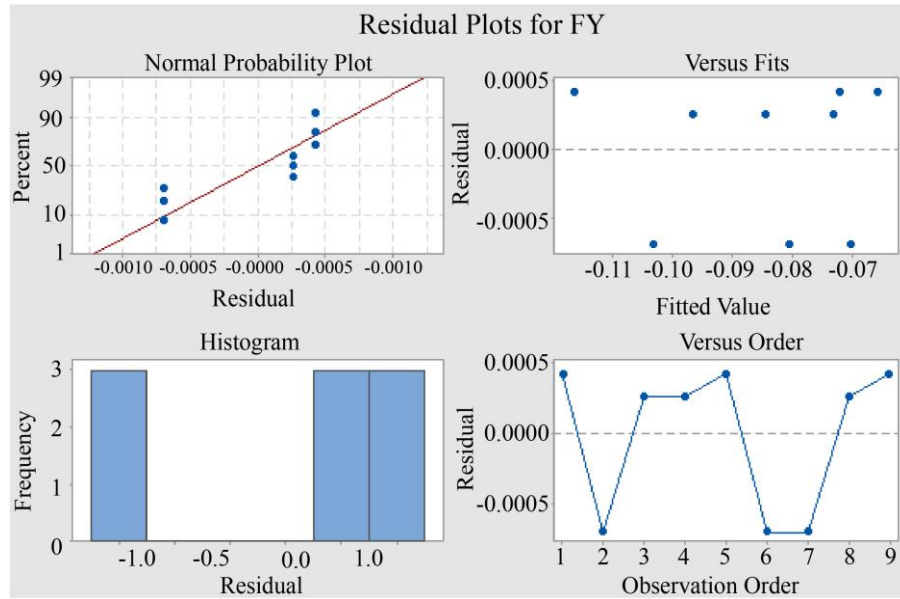
Fig. 11 Residual effects on FY

7. Conclusion

1. The machining properties of AISISS403 can be analyzed using the Taguchi L9-orthogonal array method with a TiZr21-coated tungsten carbide tool.

2. MINITAB-19 software was used to perform regression analysis, which plotted the residual effects of controlled parameters on surface roughness, FX, and FY cutting forces. Figures 7, 8, and 9 designate that all results were satisfactory and close to the mean line.

3. The ideal surface roughness value has been discovered to be attainable at 700 r.p.m. This indicates that the speed of cutting has the most important impact on RA as well as the cutting forces FX and FY. The second and third most dominant factors are feed and cut depth, respectively.

4. The best surface roughness rating was obtained with a cutting speed of 700 r.p.m., a feed rate of 0.4 mm/rev, and a depth of cut of 0.25 mm. The optimal cutting force FX value was discovered using a cutting speed of 700 r.p.m., a feed rate of 0.4 mm/rev, and a depth of cut of 0.35 mm. In contrast, the best numbers for cutting force FY were 650 r.p.m. of cutting speed, 0.4 mm/rev of feed rate, and 0.45 mm of cut depth.

References

[1] Lohithaksha M. Maiyar et al., "Optimization of Machining Parameters for end Milling of Inconel 718 Super Alloy Using Taguchi Based Grey Relational Analysis," *Procedia Engineering*, vol. 64, pp. 1276-1282, 2013. [CrossRef] [Google Scholar] [Publisher Link]

[2] Hilmi Pekşen, and Ali Kalyon, "Optimization and Measurement of Flank Wear and Surface Roughness via Taguchi Based Grey Relational Analysis," *Materials and Manufacturing Processes*, vol. 36, no. 16, pp. 1865-1874, 2021. [CrossRef] [Google Scholar] [Publisher Link]

[3] Ravi Patel, Ankit Kumar, and Jitendra Kumar Verma, "Analysis and Optimization of Surface Roughness in Turning Operation of Mild Steel Using Taguchi Method," *International Journal of Engineering Trends and Technology*, vol. 34, no. 7, pp. 337-341, 2016. [CrossRef] [Google Scholar] [Publisher Link]

[4] Arshad Noor Siddiquee et al., "Optimization of Deep Drilling Process Parameters of AISI 321 Steel Using Taguchi Method," *Procedia Materials Science*, vol. 6, pp. 1217-1225, 2014. [CrossRef] [Google Scholar] [Publisher Link]

[5] Awadhesh Pal, S.K. Choudhury, and Satish Chinchanikar, "Machinability Assessment through Experimental Investigation during Hard and Soft Turning of Hardened Steel," *Procedia Materials Science*, vol. 6, pp. 80-91, 2014. [CrossRef] [Google Scholar] [Publisher Link]

[6] M. Aramesh et al., "Survival Life Analysis of the Cutting Tools During Turning Titanium Metal Matrix Composites (Ti-MMCs)," *Procedia CIRP*, vol. 14, pp. 605-609, 2014. [CrossRef] [Google Scholar] [Publisher Link]

[7] J.A. Ghani, I.A. Choudhury, and H.H. Masjuki, "Wear Mechanism of TiN Coated Carbide and Uncoated Cermets Tools at High Cutting Speed Applications," *Journal of Materials Processing Technology*, vol. 153-154, pp. 1067-1073, 2004. [CrossRef] [Google Scholar] [Publisher Link]

[8] H. Hong et al., "Machinability of Steels and Titanium Alloys Under Lubrication," *Wear*, vol. 162-164, pp. 34-39, 1993. [CrossRef] [Google Scholar] [Publisher Link]

[9] G.K. Dosbaeva et al., "Cutting Temperature Effect on PCBN and CVD Coated Carbide Tools in Hard Turning of D2 Tool Steel," *International Journal of Refractory Metals and Hard Materials*, vol. 50, pp. 1-8, 2015. [CrossRef] [Google Scholar] [Publisher Link]

[10] D. Philip Selvaraj, P. Chandramohan, and M. Mohanraj, "Optimization of Surface Roughness, Cutting Force and Tool Wear of Nitrogen Alloyed Duplex Stainless Steel in a Dry Turning Process Using Taguchi Method," *Measurement*, vol. 49, pp. 205-215, 2014. [CrossRef] [Google Scholar] [Publisher Link]

[11] Håkan Thoors, H. Chandrasekaran, and Patrik Ölund, "Study of Some Active Wear Mechanisms in a Titanium-Based Cermet When Machining Steels," *Wear*, vol. 162-164, Part. A, pp. 1-11, 1993. [CrossRef] [Google Scholar] [Publisher Link]

[12] G.E. D'Errico, R. Calzavarini, and B. Vicenzi, "Influences of PVD Coatings on Cermet Tool Life in Continuous and Interrupted Turning," *Journal of Materials Processing Technology*, vol. 78, no. 1-3, pp. 53-58, 1998. [CrossRef] [Google Scholar] [Publisher Link]

[13] Atul Kulkarni et al., "Analysis of Cutting Temperature during Turning of SS 304 Using Uncoated and PVD Coated Carbide Inserts," *Materials Today: Proceedings*, vol. 68, no. 6, pp. 2569-2573, 2022. [CrossRef] [Google Scholar] [Publisher Link]

[14] Uttkarsh Patel et al., "Performance Evaluations of Ti-Based PVD Coatings Deposited on Cermet Tools for High-Speed Dry Finish Turning of AISI 304 Stainless Steel, *Wear*, vol. 492-493, 2022. [CrossRef] [Google Scholar] [Publisher Link]

[15] SatyanarayanaKosaraju, M. Vijay Kumar, and N. Sateesh, "Optimization of Machining Parameter in Turning Inconel 625," *Materials Today: Proceedings*, vol. 5, no. 2, pp. 5343-5348, 2018. [CrossRef] [Google Scholar] [Publisher Link]

[16] Miroslav Radovanović et al., "Taguchi Approach for the Optimization of Cutting Parameters in Finish Turning of Medical Stainless Steel," *Applied Mechanics and Materials*, vol. 809-810, pp. 153-158, 2015. [CrossRef] [Google Scholar] [Publisher Link]

[17] M. Nalbant, H. Gökkaya, and G. Sur, "Application of Taguchi Method in the Optimization of Cutting Parameters for Surface Roughness in Turning," *Materials & Design*, vol. 28, no. 4, pp. 1379-1385, 2007. [CrossRef] [Google Scholar] [Publisher Link]

[18] Yuhui Yang et al., "The Grey-Taguchi Method Analysis for Processing Parameters Optimization and Experimental Assessment of 42CrMo Steel Treated by Ultrasonic Surface Rolling," *Journal of Materials Research and Technology*, vol. 23, pp. 6244-6261, 2023. [CrossRef] [Google Scholar] [Publisher Link]